Overlay and Edge Placement Error Metrology in the Era of Stochastics

Chris A. Mack[a] & Michael E. Adel[b]
[a]Fractilia, Austin, Texas, USA
[b]Intellectual Landscapes, Zichron Ya'akov, Israel

Background: For the most advanced nodes, edge placement errors are typically dominated by stochastics, necessitating a rigorous stochastics approach to modeling and measuring edge placement errors and their contributors.
Aim: In this work, a new approach to developing an edge placement error (EPE) model useful for lot dispositioning or EPE budgeting is presented.
Approach: As an example of the proposed approach, a rigorous EPE model is developed for the case of complementary lithography, where dense lines and spaces are cut with a second patterning step. This model gives rise to the generation of an Overlay Process Window, the range of overlay errors that can be tolerated in the presence of stochastics critical dimension and placement errors of the individual layers.
Results: The resulting model uses only measurable quantities and allows the prediction of EPE-based failure rates for the purpose of lot dispositioning. One interesting outcome is that Angstrom-level changes in the 1-sigma stochastics terms produces nanometer-level changes in the overlay process window.
Conclusions: This new EPE modeling approach provides a more rigorous and accurate method for lot dispositioning and EPE budgeting than prior approaches.

Keywords: stochastics, overlay, edge placement error, EPE, line-edge roughness, linewidth roughness

1. INTRODUCTION

Historically, lithographers have divided their time between two very important pursuits: control of critical dimensions (CD) and control of overlay. In the past these tasks were often independent, since at that time process errors affecting CD did not significantly impact overlay, and vice versa. This pleasant division of labor changed in the era of low k_1, as small aberrations, stage non-idealities, and other previously second-order effects began affecting both CD and overlay in a coupled way. In the last 15 years or so we have added Edge Placement Error (EPE) to our list of concerns, the combination of CD errors and placement errors of a feature that couple to form an edge error that can ruin the performance or yield of a semiconductor device.[1] This has been especially true for multiple patterning processes such as complementary lithography.

More recently, the demands of ever-shrinking EPE budgets have been confounded by a new reality: stochastics contributions to EPE are growing rapidly.[2,3] At today's advanced nodes, stochastics can make up more than 50% of the edge placement errors on the wafer.[4] This has given rise to a need for methods to properly account for stochastics in EPE budgets. The approach developed by Mulkens[2] is widely used, but its inclusion of stochastics in not as rigorous as needed.

Additionally, stochastics considerations are needed for more than just EPE budget calculations, they are also needed when considering how to use overlay data in high volume manufacturing. There are two main classical overlay measurement use cases: lot dispositioning and correctable determination and feedback. For lot dispositioning, overlay measurements lead to an estimation (either direct or indirect) of yield loss due to overlay errors. If the predicted yield loss is too high, we rework the wafers rather than send them on for subsequent processing. For correctable feedback, overlay data is modeled and the model parameters are interpreted as correctables for the scanner: changes in scanner settings that would reduce the overlay error if the wafer(s) were to be reworked, and assumed to also improve subsequent lots. For both of

these use cases, important decisions could be improved if stochastics metrology data were incorporated properly into the decision-making process.

In this paper we will provide an example of stochastics-aware overlay + EPE lot dispositioning. The "Go, No-Go" decision for a lot will be made using the traditional scribe-line and/or in-die overlay data, but supplemented with stochastics metrology data such as local CD uniformity (LCDU) and local pattern placement error (LPPE) measurements on the individual patterning layers. Proper use of stochastics data dramatically affects our understanding of the impact of overlay errors on the probability of die failure, and thus on the disposition decision. The use of the stochastics-aware disposition approach to be presented here can benefit the fab by either reducing the number of bad wafers that are not reworked, or reducing the rework of good wafers, or both.

2. METHOD AND THEORY: AN EXAMPLE

There are many lithography layers for different technology nodes and processes where a stochastics approach to overlay and EPE analysis would be beneficial. Here we will pick one example case to illustrate our method, though it is widely applicable to all layers and use cases. In the following we will analyze a patterning step in which an EUV single patterning cut-mask is used to cut an array of lines and spaces (for example, made with self-aligned multiple patterning). We will first develop a geometric model for this example, then interpret the model from a stochastics perspective.

2.1 Geometric Overlay Model

Our geometric edge placement error pass/fail criterion will be based on measurable metrics such as CD-SEM and optical overlay data. A generic depiction of this multiple patterning test case is shown in Figure 1. An SADP (self-aligned double patterning) pair of lines and spaces is used such that the two lines and the two spaces may have different statistical properties. In our example case, only one line is at work but the two spaces to either side of that line (labeled Mandrel and Space in the figure) may be different statistically. Generalization of the approach to single patterning or self-aligned quadruple patterning (SAQP) formation of the lines and spaces will also be briefly examined below.

The geometry of Figure 1 defines four distances, labeled CD_1 – CD_4, between an edge of the cut feature and an edge of the line/space feature. Four failure mechanism scenarios may be envisaged as follows:

1. CD_1 vanishes, producing an incomplete cut of the line
2. CD_2 vanishes, producing an incomplete cut of the line
3. CD_3 vanishes, where the cut reaches the line below
4. CD_4 vanishes, where the cut reaches the line above

From symmetry, scenarios 1 and 2 will behave identically in the model we will develop below. Scenarios 3 and 4 will have an identical model, though with different input values due to the differences between the pitch/space above and the pitch/space below the line. Therefore, we will describe only scenarios 1 and 3 here.

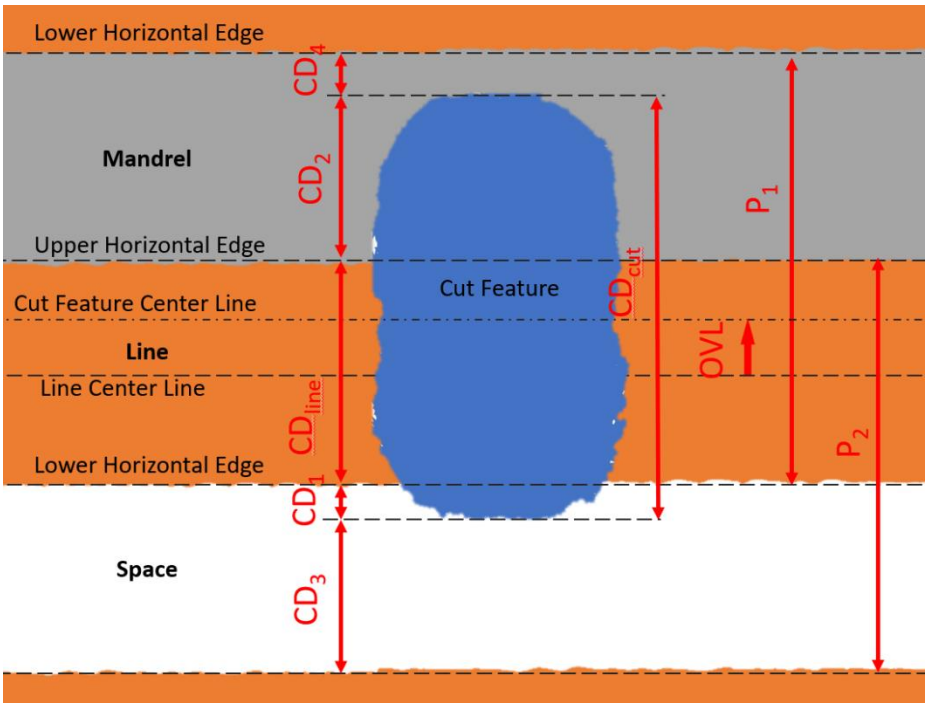

Figure 1: Geometry of a generic line/space/mandrel pattern modified by an orthogonal cut feature.

Considering scenario 1, from geometric considerations,

$$CD_1 = \frac{CD_{cut}}{2} - \frac{CD_{line}}{2} - OVL \tag{1}$$

where CD_{cut} is the vertical dimension of the cut feature, CD_{line} is the vertical width of a horizontal line and OVL is the vertical overlay error between the cut and line. We investigate failure by looking for circumstances that produce $CD_1 \leq 0$, though other CD_1 criterion could be chosen without changing the method outlined below. We will now reinterpret this geometric model as representing the mean values of distributions of CD and overlay. We will assume that each of these parameters is statistically independent and of Gaussian distributions with standard deviations $\sigma_{CD_{cut}}$, $\sigma_{CD_{line}}$, and σ_{OVL} respectively (Figure 2). Under these assumptions, σ_{CD_1}, the standard deviation of our failure mechanism parameter, may be calculated by taking the variance of equation (1):

$$\sigma_{CD_1}^2 = \frac{1}{4}\left(\sigma_{CD_{cut}}^2 + \sigma_{CD_{line}}^2\right) + \sigma_{OVL}^2 \tag{2}$$

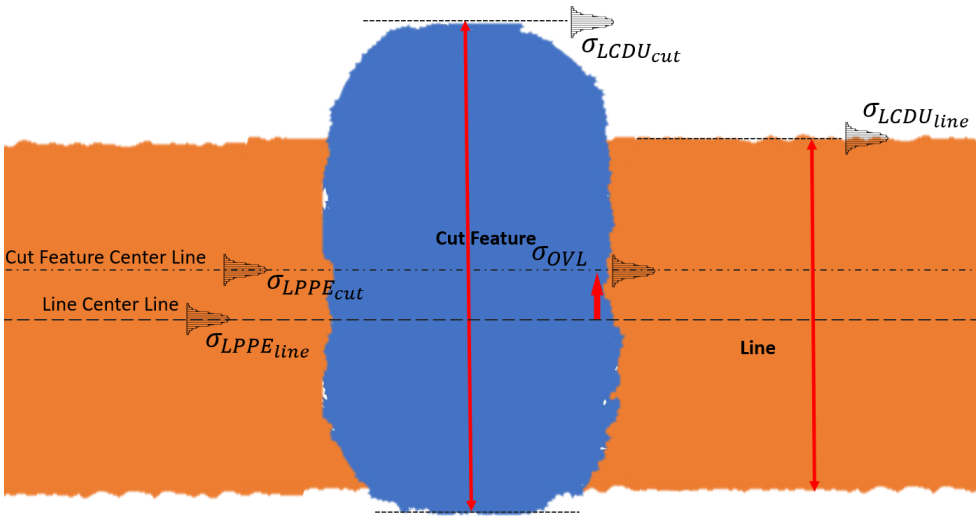

Figure 2: Stochastics parameters participating in the calculation of CD_1.

For scenario 3, from geometric considerations,

$$CD_3 = P_2 - \frac{CD_{cut}}{2} - \frac{CD_{line}}{2} + OVL = CD_{space} - \frac{CD_{cut}}{2} + \frac{CD_{line}}{2} + OVL \qquad (3)$$

where CD_{cut}, CD_{line}, and OVL and their variances are defined as above and P_2 is the pitch of the line/space pattern ($= CD_{line} + CD_{space}$). We investigate failure in this case by looking for circumstances that produce $CD_3 \leq 0$. Under these assumptions, σ_{CD_3}, the standard deviation of our failure mechanism parameter, may be calculated by the equation

$$\sigma_{CD_3}^2 = \frac{1}{4}\left(\sigma_{CD_{cut}}^2 + \sigma_{CD_{line}}^2\right) + \sigma_{OVL}^2 + \sigma_{CD_{space}}^2 + COV(CD_{line}, CD_{space}) \qquad (4)$$

where $COV(CD_{line}, CD_{space})$ is the covariance of the line and space CD, which can be related to the correlation coefficient between the line and space $COR(CD_{line}, CD_{space})$ as

$$COV\left(CD_{line}, CD_{space}\right) = \sigma_{CD_{line}}\sigma_{CD_{space}} COR\left(CD_{line}, CD_{space}\right) \qquad (5)$$

In a non-stochastic world the pitch can be assumed constant so that $\sigma_{CD_{line}} = \sigma_{CD_{space}}$ and $COR\left(CD_{line}, CD_{space}\right) = -1$. But in a world of stochastics, the left and right edges of both the line and the space can vary independently so that the pitch is not constant over the length scale of interest. If we consider the line as made up of two edge positions e1 and e2, and the space as made up of edges e2 and e3 (with shared edge e2), then

$$\begin{aligned} COV\left(CD_{line}, CD_{space}\right) &= COV(\mathrm{e2} - \mathrm{e1}, \mathrm{e3} - \mathrm{e2}) \\ = COR(\mathrm{e2}, \mathrm{e1})\sigma_{LEPE_1}\sigma_{LEPE_2} &+ COR(\mathrm{e2}, \mathrm{e3})\sigma_{LEPE_2}\sigma_{LEPE_3} \\ - COR(\mathrm{e1}, \mathrm{e3})\sigma_{LEPE_1}\sigma_{LEPE_3} &- \sigma_{LEPE_2}^2 \end{aligned} \qquad (6)$$

Thus, this term in our equation will be made up of three local edge placement error (LEPE) terms, one for each of the three line/space edges, and three correlation terms, indicating how each edge is correlated with the others.[5]

For lines and spaces printed with single patterning we expect each of the edge correlations to be near zero. Further, for uncorrelated edges with identical statistics, we expect $\sigma^2_{CD_{space}} = \sigma^2_{CD_{line}} = 2\sigma^2_{LEPE_2}$. Thus, for this case, we have

$$\begin{aligned} COR\left(CD_{line}, CD_{space}\right) &= -0.5 \\ COV\left(CD_{line}, CD_{space}\right) &= -0.5\sigma^2_{CD_{space}} \end{aligned} \tag{7}$$

For SADP $COR(\mathrm{e1}, \mathrm{e3})$ will be near zero, though this term may be non-zero for SAQP. Also for SADP, $COR(\mathrm{e2}, \mathrm{e1})$ (the correlation between the two edges of the line) may be moderately large whereas $COR(\mathrm{e2}, \mathrm{e3})$ is generally small. In any case, all of these terms are measurable and can be included in our model. For an idealized but extreme SADP case we can say that $\sigma_{LEPE_1} = \sigma_{LEPE_2}$, $COR(\mathrm{e1}, \mathrm{e3}) = COR(\mathrm{e2}, \mathrm{e3}) = 0$, and $COR(\mathrm{e2}, \mathrm{e1}) = 1$. In this case, $COV\left(CD_{line}, CD_{space}\right) = 0$. For a still idealized but more reasonable SADP case we have $COR(\mathrm{e2}, \mathrm{e1}) = 0.8$, with all other terms the same. In this case, $COV\left(CD_{line}, CD_{space}\right) = -0.2\sigma^2_{LEPE_2}$. Further, these assumptions mean that $\sigma^2_{CD_{space}} = 2 * \sigma^2_{LEPE_2}$ so that

$$COV\left(CD_{line}, CD_{space}\right) = -0.1\sigma^2_{CD_{space}} \tag{8}$$

2.2 Estimation and Interpretation of Model Parameters

While the geometric models above are straightforward, their interpretation and use require careful consideration. When applying them, for example, to a wafer or lot rework decision in the fab, inputs to the model must be interpreted statistically and supplied by measurements. Further, in a world where stochastics variations are a large (and often dominant) source of the variations of each term, their meaning and measurement are critical. Consider CD_{line}. Its variation can be broken down into global and local variations, where global variation is the classical variation wafer-to-wafer, across the wafer, and across the scanner field/slit or die. However, when interpreting failure rates, we can consider global variations as divided up between systematic signatures (fingerprints) across-wafer and across-field plus random variations.[6] The systematic signatures will be considered as offsets in the mean value of CD_{line}, while random global variations (essentially the residuals of the signatures) can be added statistically as σ_{GCDU}. Local variations are the result of stochastics. Then, the total CDU will be

$$\sigma^2_{CDU} = \sigma^2_{GCDU} + \sigma^2_{LCDU} \tag{9}$$

The local CD uniformity (LCDU) needed here is not the variation of the CD of the entire line, but the variation of a line segment of length equal to the nominal cut feature width. In other words, the variation of CD_{line} that we care about is over the region of overlap between the line and the cut. The LCDU value ($\sigma_{LCDU_{line}}$) of the segment can be measured directly using a CD-SEM, but should be unbiased by removing the impact of SEM edge detection noise.[7,8] An example is shown in Figure 3.

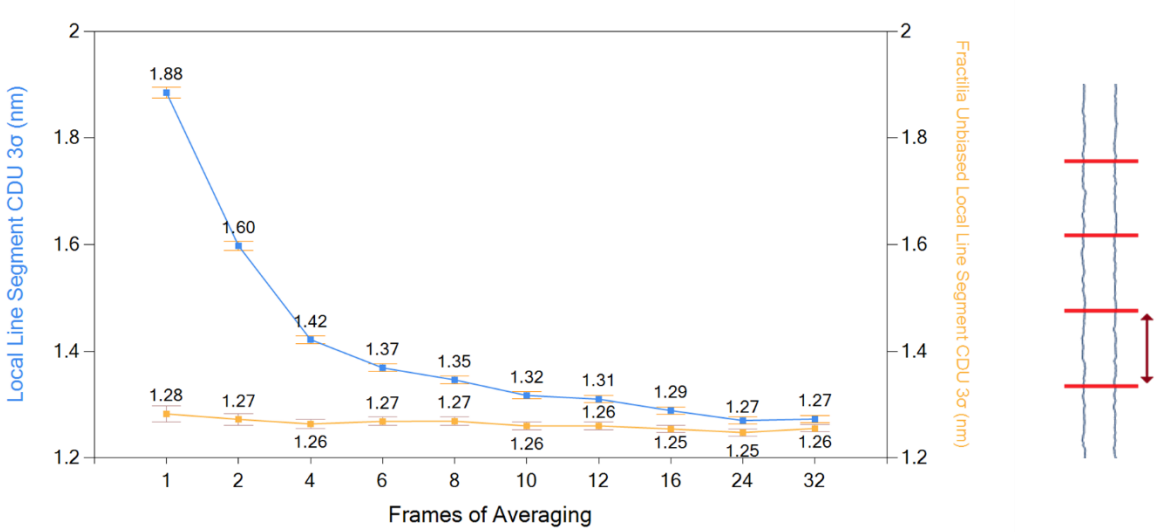

Figure 3: Biased and unbiased LCDU of a 50-nm-long line segment as a function of the number of frames of averaging in the CD-SEM. Results shown are from the 32-nm pitch after-etch line/space data of reference 8.

Alternately, the LCDU of this short line segment can be modeled based on measurement of the unbiased power spectral density (PSD) of the long line:[9]

$$\sigma_{LCDU_{line}} \approx \sigma_{LWR}\sqrt{\frac{(2H+1)\xi}{L}\left(1-\frac{\xi}{L}\right)} \qquad (10)$$

where σ_{LWR} is the LWR of the infinitely long line, L is the length of the line segment (that is, the nominal width of the cut feature), ξ is the correlation length of the LWR from the long line (as obtained from its PSD), and H is its roughness exponent. Note that equation (10) assumes $L \gg \xi$, though more exact expressions are also available.[9] In this work we will assume that $\sigma_{LCDU_{line}}$ is an unbiased measurement of the appropriate length segment.

Similarly, $\sigma_{LCDU_{cut}}$ has global and local variation components, and the local CDU of the cut in the Y-direction can be measured with a CD-SEM and unbiased (the unbiased measurement should be used in all of the equations presented here). The variation of the pitch (whether P_1 or P_2) has a global component often referred to as pitch-walking, caused by global variations in the self-aligned multiple patterning process, and represented in our case as the global variation in the space width. The local component is the local CDU of the space ($\sigma_{LCDU_{space}}$) broken down into the same short segment as used to evaluate $\sigma_{LCDU_{line}}$. As mentioned for the scenario 3, we may also need to measure the correlation between edges over a length scale equal to the width of the cut feature.

With respect to overlay, there are at least two sources of metrology data which may be used to build estimates of the mean and variance of the distribution. It has been shown by Arnold[10] that pooled overlay data at the wafer level is by no means normal in its distribution, displaying both skewness and kurtosis. Therefore, the approach proposed here is to rely on a spatially varying line-to-cut overlay model generated by optical overlay metrology. The modeled overlay will be our estimate of mean overlay $OVL(x, y)$, x and

y representing positions within the wafer, field, or die. In order to estimate the local variation of the overlay we must include the local pattern placement errors of the line and the cut.

$$OVL = OVL(x, y) + PPE_{line} + PPE_{cut} \tag{11}$$

where PPE_{line} and PPE_{cut} are the pattern placement errors of the line segment and cut feature respectively, with mean values that are typically zero or have a fixed value for a given pattern (the so-called non-zero offset)[11].

Taking the variance of equation (11),

$$\sigma_{OVL}^2 = \sigma_{Res}^2 + \sigma_{LPPE_{cut}}^2 + \sigma_{LPPE_{line}}^2 \tag{12}$$

where σ_{Res}^2 is the variance of the residuals of the overlay model $OVL(x, y)$ and LPPE is the local pattern placement error. The above relies on the assumption that each of these distributions are statistically independent from one another. This assumption is reasonable since the cut and line features are produced by separate lithographic steps and the overlay model, while produced by the overlay between those steps, is the result of metrology performed on much larger features in the scribeline. As with LCDU, LPPE of the line is measured for a segment of length equal to the width of the cut, and should be unbiased.

Combining all the sources of variations, both local and global, total variances of our failure parameters become

$$\sigma_{CD_1}^2 = \frac{1}{4}\left(\sigma_{GCDU_{cut}}^2 + \sigma_{LCDU_{cut}}^2 + \sigma_{GCDU_{line}}^2 + \sigma_{LCDU_{line}}^2\right) + \sigma_{Res}^2 + \sigma_{LPPE_{cut}}^2 + \sigma_{LPPE_{line}}^2 \tag{13}$$

$$\sigma_{CD_3}^2 = \sigma_{CD_1}^2 + \sigma_{GCDU_{space}}^2 + 0.9\sigma_{LCDU_{space}}^2 \tag{14}$$

where equation (14) makes the previously described assumptions about edge-to-edge correlations that are reasonable for an SADP case. Grouping the CDU terms from equation (13) for convenience:

$$\sigma_{CDU_1}^2 = \sigma_{GCDU_{cut}}^2 + \sigma_{LCDU_{cut}}^2 + \sigma_{GCDU_{line}}^2 + \sigma_{LCDU_{line}}^2 \tag{15}$$

gives

$$\sigma_{CD_1}^2 = \frac{1}{4}\sigma_{CDU_1}^2 + \sigma_{OVL}^2 \tag{16}$$

2.3 Predicting Failures

Our pass/fail criterion will be based on excursion count, the fraction of instances that fail to meet our specifications. To estimate this, we will rely on the cumulative distribution function assuming a Gaussian distribution, which is the fraction of cuts (*f*) that fail based on one of the criteria.

$$f(x_0, \mu, \sigma) = \frac{1}{\sqrt{2\pi}\sigma}\int_{-\infty}^{x_0} e^{-\frac{(x-\mu)^2}{2\sigma^2}} dx \tag{17}$$

where x_0 is our failure threshold, μ is the nominal (mean) value of either CD_1 or CD_3 as determined in equations (1) or (3) above, and σ^2 is the variance as defined in equations (13) or (14) above. For the case of the failure threshold set to zero,

$$f(x_0 = 0, \mu, \sigma) = \frac{1}{\sqrt{2\pi}\sigma}\int_{-\infty}^{0} e^{-\frac{(x-\mu)^2}{2\sigma^2}}dx = \frac{1}{2}erfc\left(\frac{\mu}{\sqrt{2}\sigma}\right) \quad (18)$$

In general, the fraction of failures will be small, meaning that $\mu \gg \sigma$. In this case, the complementary error function can be approximated as

$$f(x_0 = 0, \mu, \sigma) = \frac{1}{2}erfc\left(\frac{\mu}{\sqrt{2}\sigma}\right) \approx \frac{\sigma}{\sqrt{2\pi}\mu}e^{-\frac{\mu^2}{2\sigma^2}} \quad (19)$$

This approximation is off by 2.6% at a 1 part per billion failure rate, and off by 4% at the 1 part per million failure rate.

Obviously, the failure rate is controlled by σ/μ, with larger values producing greater rates of failure. For example, σ/μ = 0.167 produces a 1 part per billion failure rate, while σ/μ = 0.210 produces a 1 part per million failure rate. The exponential shape of the tail of the distribution means that small changes in σ/μ can result in large changes in the failure rate. It is also useful to express the failure rate on a log-scale. Using the approximate expression from equation (19),

$$ln(failure) \approx ln\left(\frac{\sigma}{\sqrt{2\pi}\mu}\right) - \frac{\mu^2}{2\sigma^2} \quad (20)$$

When shown on a log-scale, failure rate will vary about quadratically as μ/σ.

We can now define the σ/μ ratio for scenarios 1 and 2. The difference between the scenarios will only be the sign of the OVL term.

$$\frac{\sigma_{CD_1}}{CD_1} = \frac{\sqrt{\frac{1}{4}\sigma_{CDU_1}^2 + \sigma_{OVL}^2}}{\frac{1}{2}(CD_{cut} - CD_{line}) - OVL}, \quad \frac{\sigma_{CD_2}}{CD_2} = \frac{\sqrt{\frac{1}{4}\sigma_{CDU_1}^2 + \sigma_{OVL}^2}}{\frac{1}{2}(CD_{cut} - CD_{line}) + OVL} \quad (21)$$

Of course, failure scenarios 3 & 4 can be similarly defined.

2.4 Applying the Models

With this formalism, we can now analytically predict the excursion count (fraction of failed cuts) for a given scenario. In order to validate our formalism, we will compare the analytically predicted excursion count with the results of a stochastic simulation. For convenience, we shall normalize the data and express all results in excursions per billion (ppb).

For our study, we will use the imec N7 node (termed iN7), which is roughly equivalent to the industry 5 nm node.[12,13] While the iN7 node has a range of pitch and CD values, we will assume SAQP for 28 nm pitch equal lines and spaces, followed by EUV cut patterning using nominally 20 x 28 nm slots. Table 1 summarizes all model parameters used for simulations and calculations in the next section. Based on our experience, we have put into this table reasonable values for the global CD variation (GCDU), stochastic CD

variations (LCDU), and stochastic pattern placement variations (LPPE), though of course different processes will have different values. Nominal values for the mean CDs will be used, but global variations across the die and across the wafer would be accounted for as offsets to these nominal values.

Table 1: Default model parameters used for simulations and calculations.

Parameter name	Parameter symbol	Parameter value [nm]
Line CD	CD_{line}	14
Space CD	CD_{space}	14
Mandrel CD (same as Space CD)	CD_{space}	14
Cut CD	CD_{cut}	28
Cut extension over space	CD_1	calculated by eq. (1)
Cut extension over mandrel	CD_2	calculated by eq. (1) using opposite OVL sign
Overlay (varied)	OVL	-7 to +7
Line global CD uniformity	$\sigma_{GCDU_{line}}$	0.6
Line local CD uniformity	$\sigma_{LCDU_{line}}$	0.7
Line local pattern placement error uniformity	$\sigma_{LPPE_{line}}$	0.4
Cut global CD uniformity	$\sigma_{GCDU_{cut}}$	0.8
Cut local CD uniformity	$\sigma_{LCDU_{cut}}$	0.9
Cut local pattern placement error uniformity	$\sigma_{LPPE_{cut}}$	0.5
Space global CD uniformity	$\sigma_{GCDU_{space}}$	0.7
Space local CD uniformity	$\sigma_{LCDU_{space}}$	0.7
Mandrel global CD uniformity	$\sigma_{GCDU_{mandrel}}$	0.5
Mandrel local CD uniformity	$\sigma_{LCDU_{mandrel}}$	0.5
Overlay (model residuals)	σ_{Res}	0.8
Overlay (total standard deviation)	σ_{OVL}	calculated by eq. (12)
Cut extension over space uniformity	σ_{CD1}	calculated by eq. (13)
Cut extension over mandrel uniformity	σ_{CD2}	calculated by eq. (13)

As an outcome of this method, it will be possible to calculate the size of an "overlay process window" (OPW) at the device level, as defined below, based on actual metrology data.

3. RESULTS AND DISCUSSION

3.1 Stochastic Simulation Results

To verify the analytical expressions derived above, a stochastic simulation was performed for a test case of CD_1. One million simulation iterations were performed (with values of each term of equation (1) drawn from a Gaussian distribution) and, as expected, good matching was achieved between analytical and simulated results for the mean and standard deviation of CD_1 within the expected uncertainties. Consequently, all further results will use the analytical models.

3.2 Analytical Model Results

Using the formalism described in section 2 above, the predicted excursion counts for CD_1 and CD_2 failure mechanisms have been analytically calculated as a function of overlay for three different values of σ_{OVL} as

defined in equation (12). The results are shown in Figure 4. As expected, the CD_1 and CD_2 results display reflection symmetry about zero overlay.

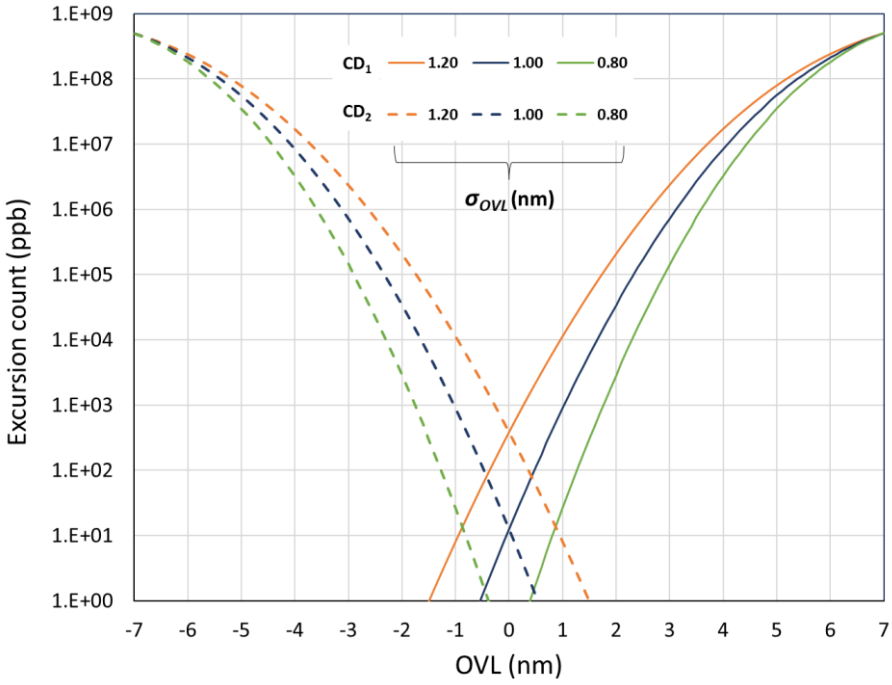

Figure 4: Log plot of the predicted excursion counts for CD_1 and CD_2 failure mechanisms as a function of overlay for three different values of σ_{OVL}, displaying the quadratic behavior expected from equation (20). $\sigma_{CDU_{cut}}$ is fixed at 1.2 nm and $\sigma_{CDU_{line}}$ is 0.92 nm.

We will define an overlay process window (OPW) as the range the overlay errors that keeps our predicted failure rate above a certain level. The sum of excursion counts for CD_1 and CD_2 as a function of overlay is shown in Figure 5, which also displays the results generated by the approximations defined in equation (19). In the regime of interest, where overlay is small, the discrepancy between the approximation and the accurate expression of equation (18) is negligible. By setting a process window boundary at 1 ppm, upon inspection of Figure 5 we can see that the OPW is about 3.5, 2 and 0.5 nanometers for the cases of σ_{OVL} = 0.8, 1.0 and 1.2 nanometers respectively. It is interesting to note that increases in the stochastics parameter σ_{OVL} on the order of Angstroms result in shrinkage of the OPW at the scale of nanometers, indicating the criticality of correctly estimating these parameters. Note that a more complete model would add scenarios 3 and 4 failure rates as well.

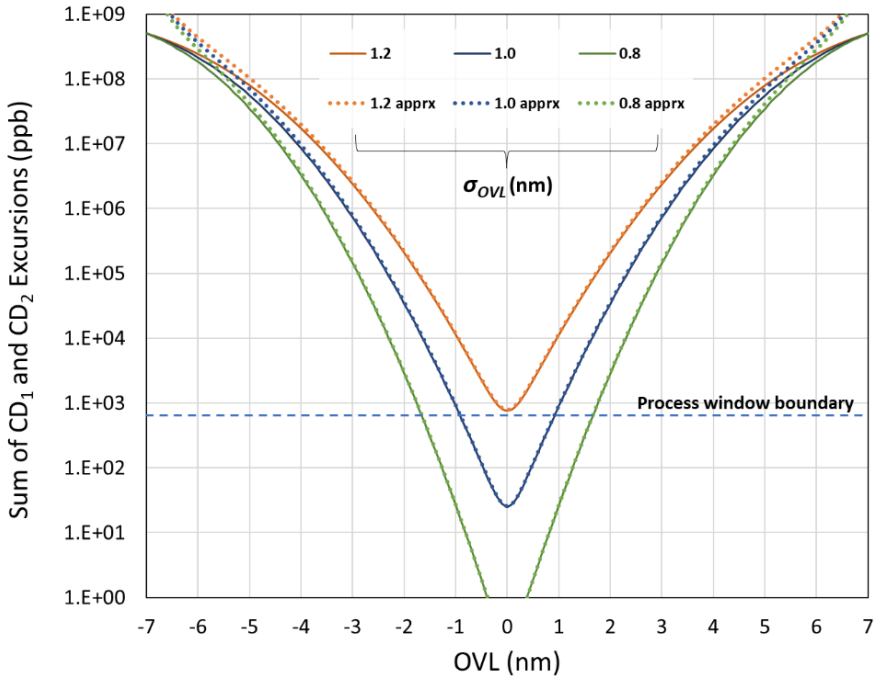

Figure 5: The solid lines display the sum of predicted CD_1 and CD_2 excursions as a function of overlay for three values of σ_{OVL} when $\sigma_{CDU_{cut}}$ is 1.2 nm and $\sigma_{CDU_{line}}$ is 0.92 nm. The dotted lines are the approximated function of equation (19). The process window boundary has been set to 1 ppm.

3.3 Overlay Process Window Results

It is instructive to quantitatively evaluate the dependence of the OPW on stochastics metrology parameters. The results are displayed in Figure 6, Figure 7, and Figure 8. The first two illustrate the OPW dependence on σ_{OVL} and $\sigma_{CDU_{cut}}$ respectively. It is noted that OPW diminishes more rapidly with σ_{OVL} than $\sigma_{CDU_{cut}}$. This is a result of the simple geometric dependence of CD_1 on OVL, CD_{cut} and CD_{line} expressed in equation (1). Figure 7 shows the OPW dependence in which σ_{OVL} remains constant at the default value of 1 nm and only the local CDU variances are varied. Unsurprisingly, the overlay process window also shrinks with increasing CD nonuniformity.

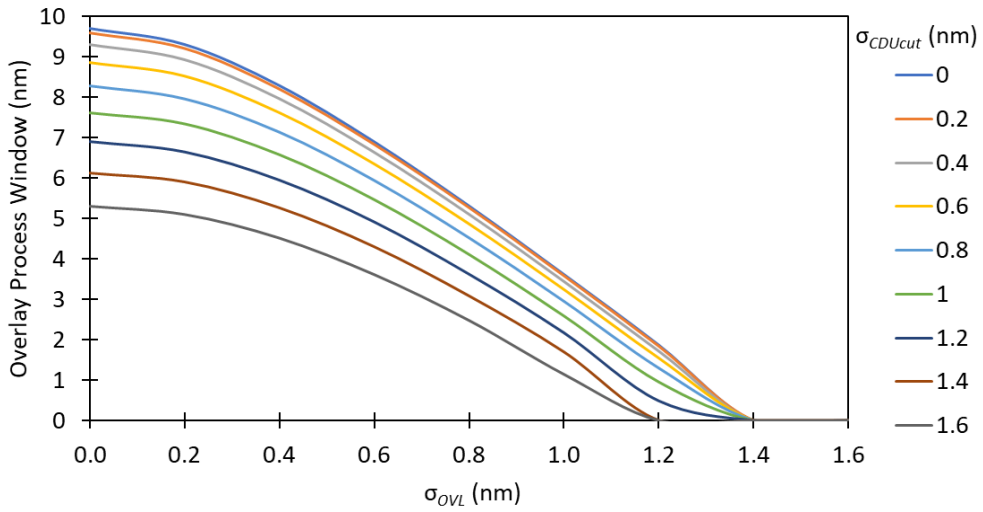

Figure 6: Overlay process window dependence on σ_{OVL} for different values of $\sigma_{CDU_{cut}}$. All other parameters as in Table 1.

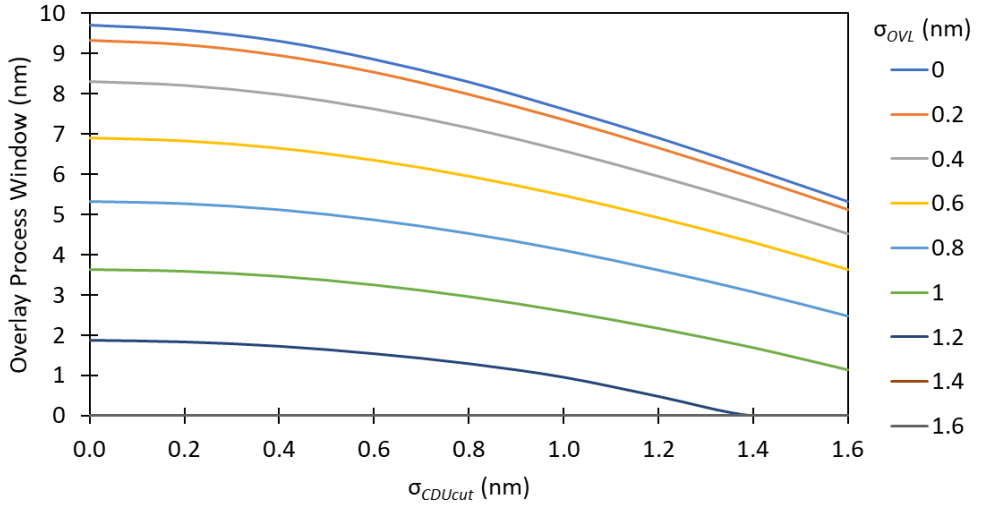

Figure 7: Overlay process window dependence on $\sigma_{CDU_{cut}}$ for different values of σ_{OVL}. All other parameters as in Table 1.

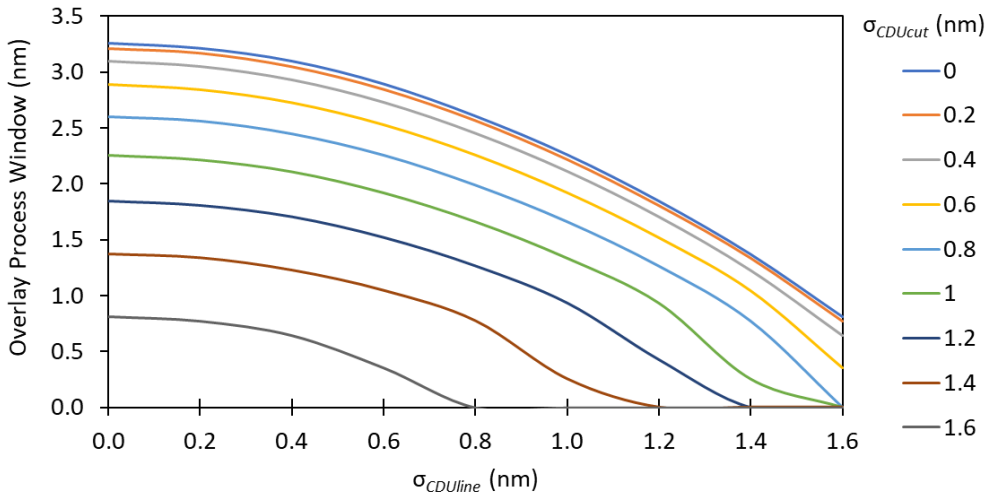

Figure 8: Overlay process window dependence on $\sigma_{CDU_{line}}$ for different values of $\sigma_{CDU_{cut}}$. All other parameters as in Table 1.

3.4 EPE Budget

Another use of the above model for EPE failure rates is for EPE budgeting. As mention above, σ/μ = 0.210 produces a 1 part per million failure rate, with the ratio σ/μ given by equation (21) for our example use case. This can be written as

$$\frac{\sigma_{CD_1}}{CD_1} = 0.21 = \frac{\sigma_{CD_1}}{CD_{1-\text{nominal}} - \Delta CD_1} \tag{22}$$

where $CD_{1-\text{nominal}}$ is the target value of CD_1 (that is, half of the nominal spacewidth) and ΔCD_1 is the total global systematic errors in CD_{cut}, CD_{line}, and OVL. Rearranging this equation, and recognizing that the maximum allowed EPE is $CD_{1-\text{nominal}}$,

$$EPE_{max} = \Delta CD_1 + \frac{\sigma_{CD_1}}{0.21} \tag{23}$$

The 0.21 factor comes from the 1 ppm failure rate spec, so that other specs will produce other multiplicative factors. In general,

$$EPE_{max} = \Delta CD_1 + k\sigma_{CD_1} \tag{24}$$

where the coverage factor k is 4.75 for the 1 ppm spec case and 6 for the 1 ppb spec, but in general will be between 3 and 7. Note that a value of 3 for the coverage factor is almost an industry standard, even though it generally does not convey the desired failure rate probability spec.

4. CONCLUSIONS

A rigorous approach to overlay lot dispositioning in the stochastics era requires more than just overlay data. Stochastic (local) variations in the individual patterning layers combine with systematic (global) variations to impact the probability of a failure. To illustrate how to combine systematic and random errors in edge placement, a specific example was chosen: the cutting of a line/space pattern to produce narrow tip-to-tip spacings in a classic complementary lithography scheme. The basic approach follows these steps.

1. Define the distance metric of interest and a failure criterion for it. In this case, we defined CD_1 as the edge overlap of the cut hole to the line being cut. Failure occurs when $CD_1 \leq 0$.
2. Using basic geometric considerations, write the equation that relates the distance metric to specific measures from each individual patterning layer and possibly the overlay between layers.
3. Interpreting each term in this equation as a random variable, take the variance of the equation. Be sure to consider correlations between terms.
4. From the variance equation, determine the wafer measurements that are required to define the magnitude of each term. In this case, the line and space CD must be interpreted as a segment CD, the segment length set to be the nominal cut feature width. Be sure to use unbiased measurements when possible.
5. Interpret systematic global variations to be shifts in the mean for each term in the equation, and random variations to be a combination of local (stochastics) variations and residuals of the systematic signatures.
6. Assuming a Gaussian distribution (though other distributions are possible), use the cumulative distribution function to define the failure probability. Set a spec for the maximum allowed failure probability.
7. The resulting equations allow for both lot dispositioning based on the predicted failure probability, or an EPE budget equation.
8. Use the resulting equations to explore control trade-offs. In this example, the overlay process window shows how changes in stochastics control affects the maximum overlay error that could be tolerated.

These steps can be followed for any patterning application, from simple to complex. Proper application yields an accurate expression using only measurable quantities.

5. REFERENCES

[1] Yan Borodovsky, "EUV Lithography at Insertion and Beyond", International Workshop on EUV Lithography, Maui, Hi (2012).

[2] Jan Mulkens, Michael Hanna, Hannah Wei, Vidya Vaenkatesan, Henry Megens, and Daan Slotboom "Overlay and edge placement control strategies for the 7nm node using EUV and ArF lithography", Proc. SPIE 9422, *Extreme Ultraviolet (EUV) Lithography VI*, 94221Q (2015).

[3] Jaeseung Jeong, Jinho Lee, Jinsun Kim, Sunyoung Yea, *et al.*, "Understanding advanced DRAM edge placement error budget and opportunities for control", Proc. SPIE 11325, *Metrology, Inspection, and Process Control for Microlithography XXXIV*, 1132506 (2020).

[4] Eric Verhoeven, Ron Schuurhuis, Marcel Mastenbroek, Peter Jonkers, *et al*., "0.33 NA EUV systems for High Volume Manufacturing", Proc. SPIE 11517, *Extreme Ultraviolet Lithography 2020*, 1151703 (2020).

[5] Vassilios Constantoudis, George Papavieros, Evangelos Gogolides, Alessandro Vaglio Pret, *et al*., "Challenges in line edge roughness metrology in directed self-assembly lithography: placement errors and cross-line correlations", *J. Micro/Nanolith. MEMS MOEMS*, **16**(2), 024001 (2017).

[6] Chris A. Mack, Fundamental Principles of Optical Lithography: The Science of Microfabrication, John Wiley & Sons, pp. 312-314, (London: 2007).

[7] Chris A. Mack, "Reducing roughness in extreme ultraviolet lithography", *Journal of Micro/Nanolithography, MEMS, and MOEMS*, **17**(4), 041006 (2018).

[8] Chris A. Mack, Frieda Van Roey, and Gian F. Lorusso, "Unbiased Roughness Measurements: Subtracting out SEM Effects, part 3", Proc. SPIE 10959, *Metrology, Inspection, and Process Control for Microlithography XXXIII*, 109590P (2019).

[9] Chris A. Mack, "Analytical Expression for Impact of Linewidth Roughness on Critical Dimension Uniformity", Journal of Micro/Nanolithography, MEMS, and MOEMS, **13**(2) (Apr-Jun, 2014) p. 020501.

[10] William H. Arnold "Overlay Simulator For Wafer Steppers", Proc. SPIE 0922, Optical/Laser Microlithography, (1 January 1988); https://doi.org/10.1117/12.968406

[11] Honggoo Lee et. al "Device overlay method for high volume manufacturing," Proc. SPIE 9778, Metrology, Inspection, and Process Control for Microlithography XXX, 97781F (18 March 2016); https://doi.org/10.1117/12.2219701

[12] Bharani Chava, David Rio, Yasser Sherazi, Darko Trivkovic, Werner Gillijns, *et al*., "Standard cell design in N7: EUV vs. immersion", Proc. SPIE 9427, Design-Process-Technology Cooptimization for Manufacturability IX, 94270E (2015).

[13] Eelco van Setten, Friso Wittebrood, Eleni Psara, Dorothe Oorschot, Vicky Philipsen, "Patterning options for N7 logic: prospects and challenges for EUV", Proc. SPIE 9661, 31st European Mask and Lithography Conference, 96610G (2015).